Nanotechnology Perceptions
ISSN 1660-6795
www.nano-ntp.com

Impact of Nickel and Cobalt Incorporation on the Band Gap of Copper Oxide Nanoparticles

Nikhil Parasar[1], Rituraj Mahanta[2], Bidhan Mohanta[1*]

[1]Department of Physics, Assam University, Silchar, 788011, Assam, India
[2]Department of Physics, Debraj Roy College (Autonomous), Golaghat 785621, Assam, India
Email: mbidhan@gmail.com

The study focuses on the change in the optical band gap of the nickel and cobalt-doped copper oxide nanoparticles and compares the same with pure copper oxide nanoparticles. Four sets of pure and doped copper oxide nanoparticles were prepared as pure copper oxide (CuO), Nickel doped copper oxide (Ni/CuO), cobalt-doped copper oxide (Co/CuO) and, nickel-cobalt co-doped (Ni-Co/CuO NPs). All the nanoparticles were prepared with a simple co-precipitation method. The samples were characterized with UV-visible spectroscopy, photoluminescence spectroscopy, and zeta potential measurement. For the calculation of optical band gap, two methods were followed, Tauc's method using UV-visible absorption spectra and photoluminescence emission. The band gap calculated with absorption spectra was found to be lower than that calculated with emission spectra. From zeta potential measurements, it was found that the copper oxide nanoparticles had more stability when incorporated with nickel. The samples were tested for the photocatalytic degradation of malachite green (MG). Increased band gap of copper oxide nanoparticles offers potential improvement in the photocatalytic activity of copper oxide nanoparticles.
Keywords: malachite green, UV-visible absorption, nanoparticles.

1. Introduction

Many studies have been carried out on metal oxide nanoparticles due to their diverse range of potential applications in medical and environmental fields [1]. Titanium oxide nanoparticles are the most used in various commercial fields. Among metal oxide nanoparticles, copper oxide, and zinc oxide nanoparticles have a comparable competence with titanium oxide nanoparticles in different fields of application [2]. With a narrow band gap of 1.2 eV, CuO nanomaterials are a favorable candidate for many industrial and

commercial applications.

With a manipulation in band gap, copper oxide nanomaterial can be used in a wide range of applications. In solar energy conversion-based applications of nanoparticles, band gap manipulation can have a large impact. For example, the use of copper oxide nanoparticles can be highly beneficial for solar cell production [3], environmental remediation [2], catalysis [4], photo-catalysis [5], water splitting [6] etc.

The band gap of any nanomaterial can be manipulated by changing some parameters in its synthesis mechanism such as temperature, pH value, doping concentration, etc. [7], [8]. The p-type semiconductor material CuO can also be manipulated into n-type by doping the material with proper metal dopants [9]. The variation in doping concentration can change the charge carrier mobility. This changes the optical properties of CuO NPs as well as the other properties with higher amplitude [10], [11]. The incorporation of transition metals like cobalt (Co), nickel (Ni), etc. in the crystal structure of host CuO, can vary the ionic radii and valence state of CuO. This results in the generation of cation and anion vacancies in the CuO lattice [12], [13], [14], [15].

Many research works have been conducted on the doping of CuO with alkali metals [16], [17], lanthanide ions [18], transition metals [19], etc. Alkali metal-doped CuO NPs increase the optical band gap with increased doping concentration [16]. Incorporating Na^+ ions in CuO lattice creates copper vacancies due to charge variation [20]. In the present work, changes in the optical band gap of CuO NPs have been studied with nickel and cobalt incorporation.

2. Synthesis of pure and (Co, Ni)-doped CuO Nanostructures:

Materials Used: The main precursor of copper nanoparticles was the copper acetate monohydrate [Cu $(CO_2CH_3)_2$. H_2O] (99% pure). Potassium hydroxide (KOH) was used as the reducing agent. Polyethylene glycol (PEG)-400 was used as the capping and stabilizing agent in the solution during reflux. All the chemicals were analytical-grade reagents that were used without further purification. For doping of nickel and cobalt, nickel chloride hexahydrate and cobalt acetate tetrahydrate were used respectively. For the photocatalytic experiment, malachite green (MG) dye was used.

Experimental procedure: A one-molar solution of [Cu $(CO_2CH_3)_2$. H_2O] was prepared using de-ionized water. The solution was kept under constant stirring at 80^{o}C temperature. A previously prepared KOH solution of the same molar concentration was added drop wise to the above solution. The pH level of the mixture was kept at 9. A distinct colour change from blue to dark brown was noticed after sometime. A small amount of PEG-400 was added dropwise to the mixture solution. For nickel and cobalt doping 2, 4, 6 mol% of nickel chloride hexahydrate and cobalt acetate tetrahydrate were added in the above solution during reflux. A homogenous mixture was formed. After 3.5 h of reflux, a black precipitate was observed. This precipitate was filtered out and centrifuged with de-ionized water for several times. Then it was kept in a hot air oven at 100^{o}C overnight and finally calcinated at 400^{o}C in a muffle furnace for 3h. The final yield was a black powder. In this procedure, four sets of nanoparticles were prepared as pure copper oxide (CuO), nickel-doped copper oxide

(Ni/CuO), cobalt-doped copper oxide (Co/CuO) and nickel, cobalt co-doped (Ni, Co/CuO).

Characterizations: The UV-visible absorption spectra of the samples were recorded using a UV-Vis spectrophotometer (Model: 2600i, Shimadzu). Photoluminescence emission spectra were collected from a photoluminescence spectrometer (Cary Eclipse Agilent). Zeta potential measurements were carried out with the help of the Zetasizer Nano ZSP (ZEN 5600).

3. Results and discussion:

UV-Vis Absorption Spectroscopy:

UV-Vis absorption spectra of pure and doped copper oxide nanoparticles are shown in Fig. 1. Recent literature shows that the UV-Vis absorption peak of various transition metal doped copper oxide nanoparticles is around 350 nm [21]. It was seen that, with doping the absorption peak position changes. The undoped copper oxide sample had an absorption maximum at 349 nm. After nickel doping and cobalt doping in CuO samples, the absorption peaks red-shifted to 373 nm and 390 nm respectively. From this observation, it can be concluded that the particle size of the samples increases after nickel and cobalt incorporation. Interestingly, nickel and cobalt co-doping exceptionally produced a blue shift in the absorption maxima. This signifies the smaller particle size.

The corresponding band gap of the samples is shown in Fig 2. The band gap of the samples was calculated with Tauc's method using the UV-Visible absorption values. The optical band gap of the samples was found as 1.6 eV, 1.69 eV, 1.49 eV, and 1.31 eV for pure CuO, Ni/CuO, Co/CuO, and Ni, Co/CuO respectively.

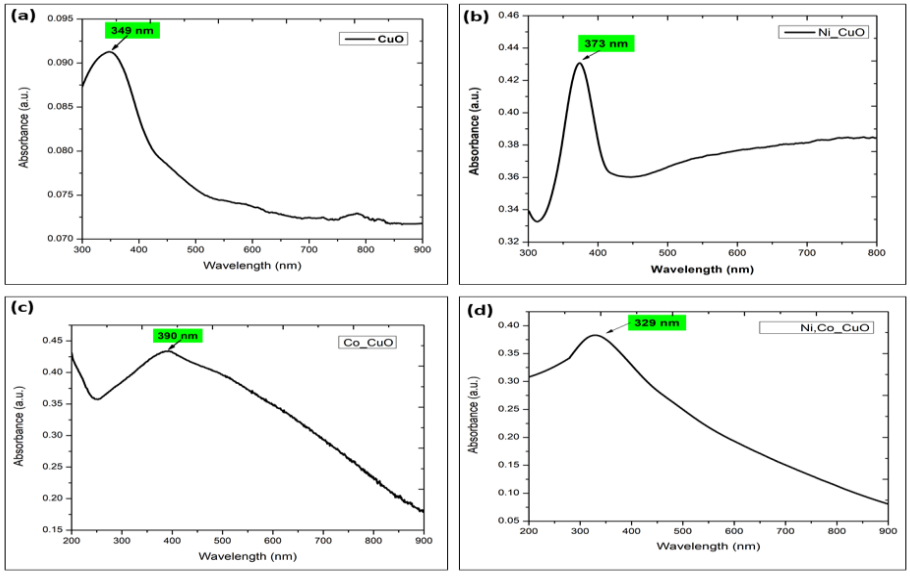

Figure 1: UV-Vis absorption spectra of (a)CuO, (b)Ni/CuO, (c)Co/CuO NPs and (d) Ni,Co/CuO NPs

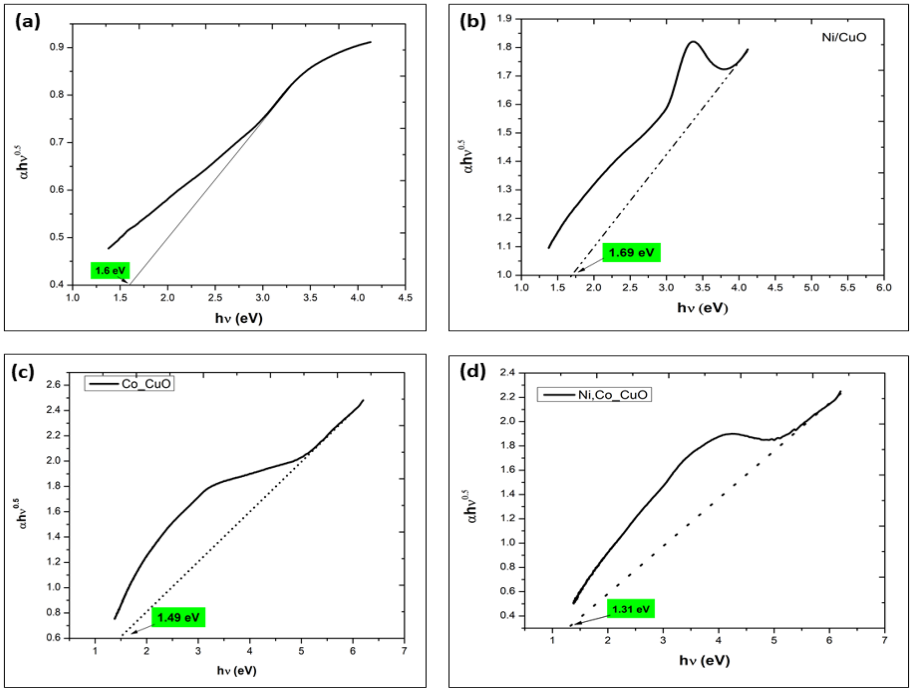

Figure 2: Optical band gap measured by Tauc's method for (a) CuO NPs, (b)Ni/CuO NPs, (c)Co/CuO NPs and (d) Ni,Co/CuO NPs

Photoluminescence spectroscopy:

PL analysis was performed for all four undoped and doped CuO NPs at different excitation levels. The variation in PL spectra of all chemically synthesized copper oxide nanoparticles is shown in Fig. 3 and Fig. 4. For the excitation wavelength at 350 nm, all samples of CuO NPs show three prominent emission peaks around 462 nm, 487 nm, and 566 nm. With nickel doping a minor blue shift is observed and with cobalt doping a minor red shit is observed near the peak at 462 nm. This may be due to the variation of the size of the particles after doping. However, two prominent emission peaks are observed at 546 nm and 573 nm for excitation at 430 nm. CuO nanomaterials show fluorescence emission around 450 nm and 530 nm corresponding to blue and green emissions respectively [22], [23]. The peak around 450 nm usually appears due to the artifacts while the other peak around 530 nm occurs due to the presence of singly ionized oxygen vacancy [24], [25]. In this experiment, the shift of the emission peak may signify the production of more oxygen vacancy in the doped CuO samples.

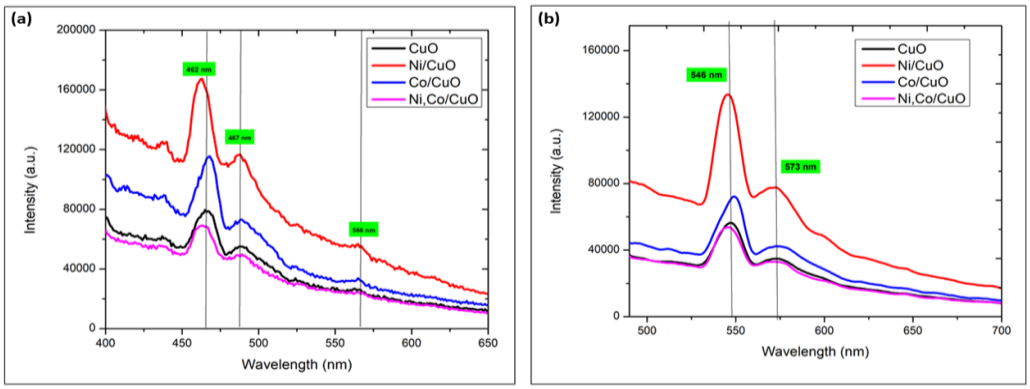

Figure 3: PL spectra of the samples with excitation at (a) 350 nm, and (b) 430 nm.

Table 1: Calculation of band gap with UV-Vis absorption spectra and photoluminescence spectra

Sample	Band gap from UV-Vis Absorption spectra (eV)	Band gap from PL Emission spectra (eV)	
		Excitation at 350 nm	Excitation at 430 nm
CuO	1.6	2.19	2.16
Co/CuO	2.36	2.21	2.27
Ni/CuO	2.55	2.54	2.47
Co, Ni/CuO	2.86	2.68	2.59

Zeta Potential Measurement:

The stability of the nanoparticles is studied with zeta potential. The results of zeta potential measurements of all the samples are shown in Fig.4. The samples show higher stability with greater zeta potential value. This happens due to the coulomb repulsion between the particles [26]. The obtained zeta potentials the shown in Table 2. The CuO nanoparticle surface has a net negative charge, likely due to the presence of hydroxyl (-OH) groups, oxygen vacancies, etc. The negative zeta potential of CuO NPs may enhance their catalytic activity [27].

The nickel-doped copper oxide nanoparticles have higher stability in suspension than the other samples as it has more negative zeta potential.

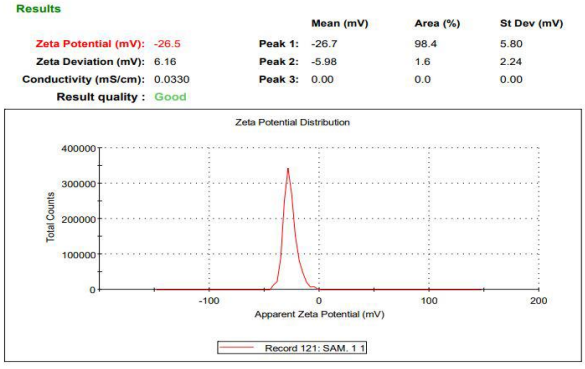

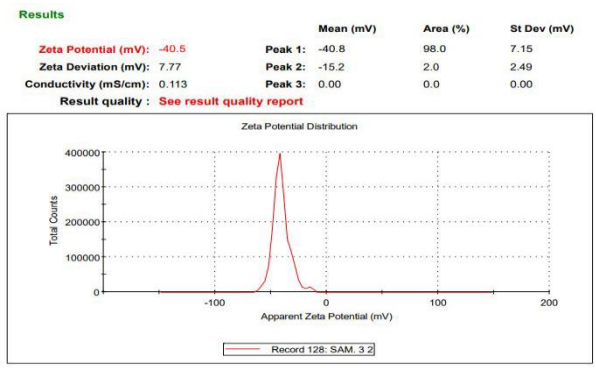

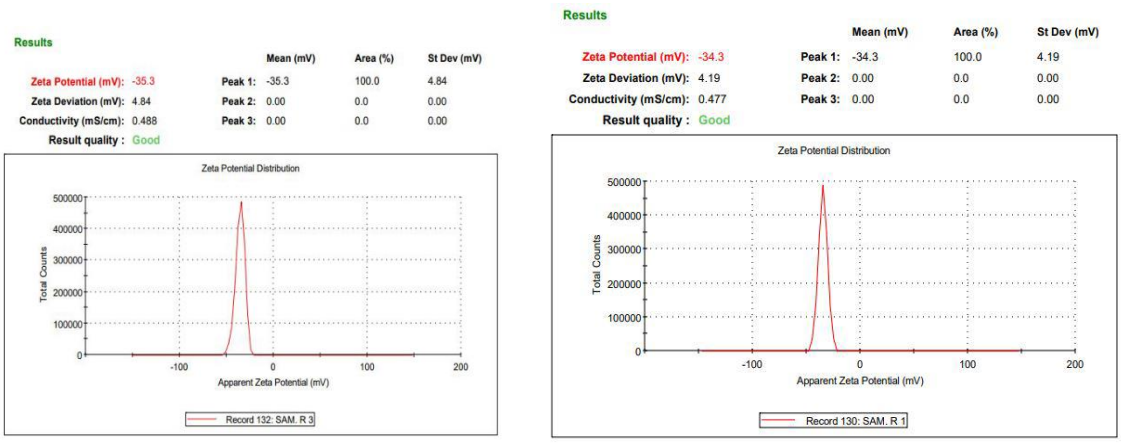

Figure 4: Zeta potential measurement result of (a) CuO NPs, (b) Ni/CuO NPs, (c) Co/CuO NPs and (d) Ni, Co/CuO NPs

Table 2: Zeta potential values of the nanoparticles

Sl. No.	Sample	Zeta Potential (mV)
1	CuO	-26.5
2	Ni/CuO	-40.8
3	Co/CuO	-34.3
4	Ni, Co/CuO	-35.3

Photocatalytic activity:

In order to check the photocatalytic activity of the samples, degradation of malachite green dye in presence of the synthesized nanoparticles was studied. About 5 mg of the synthesized samples was mixed with 1 ppm of MG dye solution. The mixture was kept under a visible light source under vigorous stirring. Four samples were collected in 30-minutes intervals and studied with UV-visible spectroscopy. The UV-visible absorption spectra during the degradation process are shown in Fig. 5. As Ni/CuO NPs had greater suspension stability than the other nanoparticles, this was used as a photocatalyst for the dye degradation test. Chemically synthesized Ni/CuO NPs effectively degraded the dye by 62.5 % in 90 min.

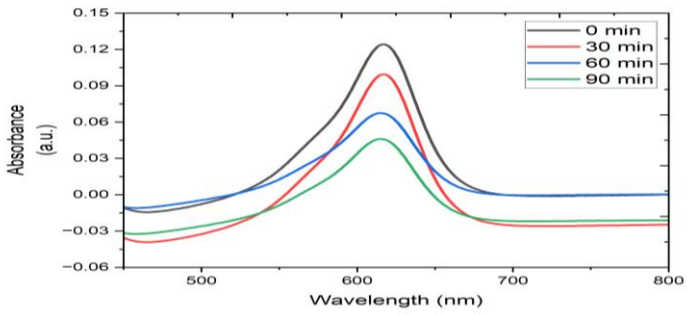

Figure 5: UV-visible absorption spectra of MG dye during photocatalytic degradation with Ni/CuO NPs as photocatalyst

4. Conclusion:

Four different sets of copper oxide nanoparticles were successfully prepared with the co-precipitation method. The optical band gap of all the nanoparticles was calculated with UV-visible absorption spectra and photoluminescence emission spectra. From both techniques, the band gap of all the samples was found in the semiconductor range. However, the result obtained with absorption spectra was more likely to be acceptable as per the literature. The band gap calculated from emission spectra was almost the same for all the nanoparticles. Nickel-doped copper oxide nanoparticles were more promising for semiconductor-based applications such as photocatalysis.

References

[1] N. Khlifi, C. Zerrouki, N. Fourati, H. Guermazi, and S. Guermazi, "Investigation of structural and optical properties of TM-doped CuO NPs: Correlation with their photocatalytic efficiency in sunlight-induced pollutant degradation," Measurement, vol. 237, p. 115209, Sep. 2024, doi: 10.1016/j.measurement.2024.115209.

[2] K. Banerjee and P. Thiagarajan, "A Review of Titanium Di Oxide Nanoparticles - Synthesis, Applications and Toxicity Concerns," Nanoscience &Nanotechnology-Asia, vol. 4, no. 2, pp. 132–143, May 2015, doi: 10.2174/2210681204666141117234425.

[3] M. H. Saleem, U. Ejaz, M. Vithanage, N. Bolan, and K. H. M. Siddique, "Synthesis, characterization, and advanced sustainable applications of copper oxide nanoparticles: a review," Clean Technol Environ Policy, Mar. 2024, doi: 10.1007/s10098-024-02774-6.

[4] B. D. Harishchandra et al., "Copper Nanoparticles: A Review on Synthesis, Characterization and Applications," Asian Pacific Journal of Cancer Biology, vol. 5, no. 4, pp. 201–210, Dec. 2020, doi: 10.31557/apjcb.2020.5.4.201-210.

[5] A. Waris et al., "A comprehensive review of green synthesis of copper oxide nanoparticles and their diverse biomedical applications," Inorg Chem Commun, vol. 123, p. 108369, Jan. 2021, doi: 10.1016/j.inoche.2020.108369.

[6] V. Dhiman, S. Singh, V. Srivastava, S. Garg, and A. D. Saran, "Nanomaterials for photo-electrochemical water splitting: a review," Environmental Science and Pollution Research, Oct. 2023, doi: 10.1007/s11356-023-30629-y.

[7] A. Pramothkumar, N. Senthilkumar, K. C. Mercy Gnana Malar, M. Meena, and I. Vetha Potheher, "A comparative analysis on the dye degradation efficiency of pure, Co, Ni and Mn-doped CuO nanoparticles," Journal of Materials Science: Materials in Electronics, vol. 30, no. 20, pp. 19043–19059, Oct. 2019, doi: 10.1007/s10854-019-02262-4.

[8] K. Deepa and T. V. Venkatesha, "Synthesis and Generation of CuO and Mn Doped CuO Composites and its Corrosion Behaviour," Mater Today Proc, vol. 4, no. 11, pp. 12045–12053, 2017, doi: 10.1016/j.matpr.2017.09.129.

[9] B. M. Abu-Zied, S. M. Bawaked, S. A. Kosa, and W. Schwieger, "Impact of Gd-, La-, Nd- and Y-Doping on the Textural, Electrical Conductivity and N2O Decomposition Activity of CuO Catalyst," Int J Electrochem Sci, vol. 11, no. 3, pp. 2230–2246, 2016, doi: 10.1016/S1452-3981(23)16097-4.

[10] C.-Y. Chiang, Y. Shin, and S. Ehrman, "Li Doped CuO Film Electrodes for Photoelectrochemical Cells," J Electrochem Soc, vol. 159, no. 2, pp. B227–B231, Jan. 2011, doi: 10.1149/2.081202jes.

[11] C.-Y. Chiang, Y. Shin, and S. Ehrman, "Dopant Effects on Copper Oxide Photoelectrochemical Cell Water Splitting," Energy Procedia, vol. 61, pp. 1799–1802, 2014, doi: 10.1016/j.egypro.2014.12.216.

[12] M. Chuai, Q. Zhao, T. Yang, Y. Luo, and M. Zhang, "Synthesis and ferromagnetism study of Ce doped CuO dilute magnetic semiconductor," Mater Lett, vol. 161, pp. 205–207, Dec. 2015, doi: 10.1016/j.matlet.2015.08.075.

[13] H. Faiz et al., "Microstructural and optical properties of dysprosium doped copper oxide thin films fabricated by pulsed laser deposition technique," Journal of Materials Science: Materials in Electronics, vol. 27, no. 8, pp. 8197–8205, Aug. 2016, doi: 10.1007/s10854-016-4824-7.

[14] D. Wang, Y. Wang, T. Jiang, H. Jia, and M. Yu, "The preparation of M (M: Mn2+, Cd2+, Zn2+)-doped CuO nanostructures via the hydrothermal method and their properties," Journal of Materials Science: Materials

in Electronics, vol. 27, no. 2, pp. 2138–2145, Feb. 2016, doi: 10.1007/s10854-015-4003-2.
[15] C. T. Meneses, J. G. S. Duque, L. G. Vivas, and M. Knobel, "Synthesis and characterization of TM-doped CuO (TM=Fe, Ni)," J Non Cryst Solids, vol. 354, no. 42–44, pp. 4830–4832, Nov. 2008, doi: 10.1016/j.jnoncrysol.2008.04.025.
[16] H. Siddiqui, M. S. Qureshi, and F. Z. Haque, "pH-Dependent Single-Step Rapid Synthesis of CuO Nanoparticles and Their Optical Behavior," Opt Spectrosc, vol. 123, no. 6, pp. 903–912, Dec. 2017, doi: 10.1134/S0030400X17120013.
[17] Mohd. Nasir et al., "Role of compensating Li/Fe incorporation in Cu 0.945 Fe 0.055−x Li x O: structural, vibrational and magnetic properties," RSC Adv, vol. 7, no. 51, pp. 31970–31979, 2017, doi: 10.1039/C7RA03960C.
[18] B. M. Abu-Zied, S. M. Bawaked, S. A. Kosa, and W. Schwieger, "Impact of Gd-, La-, Nd- and Y-Doping on the Textural, Electrical Conductivity and N2O Decomposition Activity of CuO Catalyst," Int J Electrochem Sci, vol. 11, no. 3, pp. 2230–2246, 2016, doi: 10.1016/S1452-3981(23)16097-4.
[19] D. Wang, Y. Wang, T. Jiang, H. Jia, and M. Yu, "The preparation of M (M: Mn2+, Cd2+, Zn2+)-doped CuO nanostructures via the hydrothermal method and their properties," Journal of Materials Science: Materials in Electronics, vol. 27, no. 2, pp. 2138–2145, Feb. 2016, doi: 10.1007/s10854-015-4003-2.
[20] R.-C. Wang, S.-N. Lin, and J. Liu, "Li/Na-doped CuO nanowires and nanobelts: Enhanced electrical properties and gas detection at room temperature," J Alloys Compd, vol. 696, pp. 79–85, Mar. 2017, doi: 10.1016/j.jallcom.2016.11.214.
[21] K. C. M. G. Malar, M. B. A. Titlin, R. Venkatesh, S. Keerthana, and C. R. Dhas, "Versatile effects of transition metal-doped copper oxide nanoparticles on the efficacy of photocatalytic and antimicrobial activity," J Mater Res, vol. 37, no. 23, pp. 4045–4058, Dec. 2022, doi: 10.1557/s43578-022-00762-4.
[22] R. A. Zarate, F. Hevia, S. Fuentes, V. M. Fuenzalida, and A. Zúñiga, "Novel route to synthesize CuO nanoplatelets," J Solid State Chem, vol. 180, no. 4, pp. 1464–1469, Apr. 2007, doi: 10.1016/j.jssc.2007.01.040.
[23] P. Huh, J. Yang, and S.-C. Kim, "Facile formation of nanostructured 1D and 2D arrays of CuO islands," RSC Adv, vol. 2, no. 13, p. 5491, 2012, doi: 10.1039/c2ra20097j.
[24] P. Chand, A. Gaur, and A. Kumar, "Structural, optical and ferroelectric behavior of CuO nanostructures synthesized at different pH values," Superlattices Microstruct, vol. 60, pp. 129–138, Aug. 2013, doi: 10.1016/j.spmi.2013.04.026.
[25] H. Siddiqui, M. S. Qureshi, and F. Z. Haque, "One-step, template-free hydrothermal synthesis of CuO tetrapods," Optik (Stuttg), vol. 125, no. 17, pp. 4663–4667, Sep. 2014, doi: 10.1016/j.ijleo.2014.04.090.
[26] S. Kriegseis, A. Y. Vogl, L. Aretz, T. Tonnesen, and R. Telle, "Zeta potential and long-term stability correlation of carbon-based suspensions for material jetting," Open Ceramics, vol. 4, p. 100037, Nov. 2020, doi: 10.1016/j.oceram.2020.100037.
[27] B. Liu, Y. Li, S. Qing, K. Wang, J. Xie, and Y. Cao, "Engineering CuO x –ZrO 2 –CeO 2 nanocatalysts with abundant surface Cu species and oxygen vacancies toward high catalytic performance in CO oxidation and 4-nitrophenol reduction," CrystEngComm, vol. 22, no. 23, pp. 4005–4013, 2020, doi: 10.1039/D0CE00588F.